International Journal of Chemical, Materials and Biomolecular Sciences
ISSN: 2415-6620
Vol:6, No:10, 2012

Simulation of Reactive Distillation: Comparison of Equilibrium and Nonequilibrium Stage Models

Asfaw Gezae Daful

Abstract—In the present study, two distinctly different approaches are followed for modeling of reactive distillation column, the equilibrium stage model and the nonequilibrium stage model. These models are simulated with a computer code developed in the present study using MATLAB programming. In the equilibrium stage models, the vapor and liquid phases are assumed to be in equilibrium and allowance is made for finite reaction rates, where as in the nonequilibrium stage models simultaneous mass transfer and reaction rates are considered. These simulated model results are validated from the experimental data reported in the literature. The simulated results of equilibrium and nonequilibrium models are compared for concentration, temperature and reaction rate profiles in a reactive distillation column for *Methyl Tert Butyle Ether* (MTBE) production. Both the models show similar trend for the concentration, temperature and reaction rate profiles but the nonequilibrium model predictions are higher and closer to the experimental values reported in the literature.

Keywords—Reactive Distillation, Equilibrium model, Nonequilibrium model, *Methyl Tert-Butyl Ether*

I. Introduction

REACTIVE distillation is a separation process that combines both chemical reaction and distillation in a single unit. It is gaining importance for the synthesis of reversible or consecutive chemical reactions for exceeding the equilibrium conversion and reducing the rate of formation of byproducts. These products must be removed from the column, by distillation, to increase the efficiency of the system[1–5]. Reactive distillation is attractive when the reactant-product component relative volatilities allow recycle of reactants into the reactive zone via rectification/stripping and sufficiently high reaction rates can be achieved at tray bubble temperature[5–7]. For equilibrium limited reactions, the continuous removal of products drives the reaction to near completion. Huss *et. al.*[8] show the reaction can also significantly simplify the separation task by reacting away azeotropes. M. El-Halwagi *et. al.*[9] and San-Jang Wang *et. al.*[10] recently proposed an intensified schemes to reduce energy requirements and equipment costs in reaction-separation processes. Reactive distillation process involving multicomponent reactive separation or heterogeneously catalyzed processes are further modeled using equilibrium and nonequilibrium stage models[1–7, 11–14], nonequilibrium cell models[2] or dusty fluid model[4]. Hence, the design and operation issues for reactive distillation systems are considerably more complex than those involved for conventional reactors or distillation columns. The introduction of an on-line separation function within the reaction zone leads to complex interactions between vapor-liquid equilibrium, vapor-liquid mass transfer, intra-catalyst diffusion and chemical kinetics. The integration of the reaction and separation units leads to the substantial reduction of capital expenditure, energy requirement reduction and emissions to the environment[9, 10]. Number of research publications is greatly increasing in the field of feasibility of reactive distillation operation[15–17] process design[18], steady state multiplicities[12, 19] and modelling and simulation [4, 19, 20]. Most of these papers focused on real chemical systems, and every system had its own set of complexities in vapor-liquid equilibrium nonideality (azeotropes), reaction kinetics, and physical properties, *etc*. The discrete nature of chemical species and specific complexities in the vapor-liquid equilibrium seems to cloud the picture in understanding reactive distillation processes.

Dr. Asfaw Gezae Daful, is an Assistant Professor and Chair for Process Engineering and Industrial Technology in the School of Chemical & Bio Engineering, Addis Ababa Institute of Technology, Addis Ababa University, P. O. Box 385, Addis Ababa, Ethiopia. e-mail: agezae@gmail.com. Tel: +251 926847907

In this article, an attempt has been made to understand the complex system and to simulate equilibrium and nonequilibrium models for a quaternary reaction ($A + B \rightleftharpoons C + D$) systems. Detailed model are developed and simulated using Matlab program. A *Methyl Tert Butyl Ether* (MTBE) synthesis is used as a model system to demonstrate the approach. Concentration, temperature, and reaction rate profiles are analyzed and compared for equilibrium and nonequilibrium models. Sensitivity analysis is made for the effects of methanol feed location, and effect of reflux ratio on Isobutene Conversion.

II. Equilibrium Model

The equilibrium stage model has been generally applied to the conventional distillation, where the system is either non-reactive or associated with a simple chemical reaction[21]. Its application for reactive distillation has been discussed afterwards by Taylor and Krishna[22]. The equilibrium stage model divides the column into artificial segments. Equilibrium-based model assumes that the leaving liquid and vapor streams are at thermodynamic equilibrium for each stage. These models can be coupled with the assumption of chemical equilibrium at each stage. The kinetics can be described using an n^{th} order kinetic reaction model. The MESH-equations (Material, Equilibrium, Summation and Heat equations) are known to model equilibrium stages. Detailed analysis are given on this issue in references[21–23].

III. Non-Equilibrium Model

A typical setup considered for reactive distillation column[12] and the schematic representation of the nonequi-

librium model are shown in Fig. 1 and Fig. 2 respectively. The nonequilibrium model used in the present study for reactive distillation considers both reaction rates and mass transfer fluxes. It is assumed that bulk phase of vapor and liquid are well mixed and the mass transfer resistances are located in films near the interface. A penetration model description is used for predicting mass transfer rates. A chemical reaction term is incorporated in the model equations for generic stage k (tray or packing) and component i. The model uses the height of packing and treats the column as a continuous element.

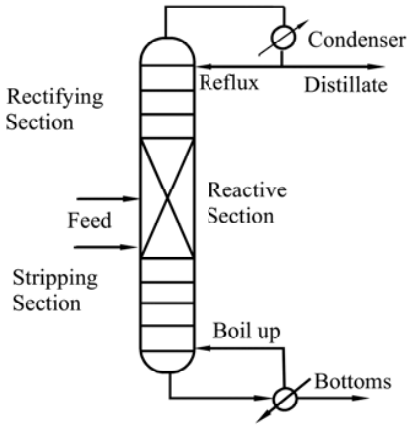

Fig. 1. Hybrid reactive distillation column for ether synthesis

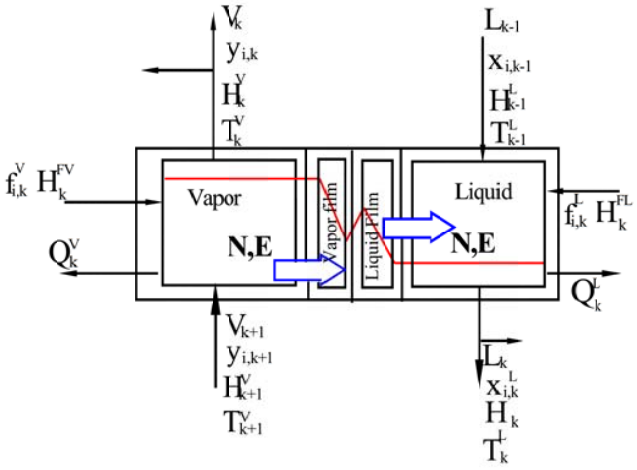

Fig. 2. Nonequilibrium stage model for pseudo homogeneous reaction in the liquid phase

The model formulation can deal with any number of reactions and the component molar balance for vapor (V) and liquid phases (L) are:

$$(1 + r_j^V)V_j y_{j,i} - V_{j+1}y_{j+1,i} - f_{j,i}^V + N_{j,i}^V = 0 \quad (1)$$

$$(1+r_j^L)L_j x_{j,i} - L_{j-1}x_{j-1,i} - f_{j,i}^L - N_{j,i}^L - \varepsilon_j \sum_{m=1}^{r} v_{m,i}R_{m,j} = 0 \quad (2)$$

Overall phase material balances are obtained by adding Eq. (1) and Eq. (2), over $i = 1$ to $i = C$, where C is the number of components, x is the mole fraction in liquid phase and y is the mole fraction in vapor phase, N is the mass transfer rate and R is the reaction rate and j represents the stage number and r_j is the ratio of side stream flow rate (S) to inter stage flow rate as, $r_j^V = \frac{S_j^V}{V_j}$ and $r_j^L = \frac{S_j^L}{L_j}$.

Summations of the component molar balance equations are also expressed for both vapor and liquid control volumes.

$$V_{j+1} - V_j + F_j^V - \sum_{i=1}^{C} N_{j,i} = 0 \quad (3)$$

$$L_{j-1} - L_j + F_j^L + \sum_{i=1}^{C} N_{j,i} + \sum_{i=1}^{C}\sum_{m=1}^{r} v_{m,i}R_{m,j}\varepsilon_j = 0 \quad (4)$$

The feed entering the column at any inlet is treated as follows: the vapor portion of this feed enters the stage above and the liquid portion of the feed enters the tray below. The feed flow rate of component i in the vapor phase to stage j is $Z_{j,i}^V F_{j,i}^V$ and in the liquid phase to stage j is $Z_{j,i}^L F_{j,i}^L$, where $Z_{j,i}^V$ and $Z_{j,i}^L$ are the corresponding mole fraction of the feed streams. The non equilibrium model uses two sets of rate equations ($\mathbf{R}$) for each stage

$$\mathbf{R}_{j,i}^V = \mathbf{N}_{j,i} - \mathbf{N}_{j,i}^V = 0 \quad (5)$$

$$\mathbf{R}_{j,i}^L = \mathbf{N}_{j,i} - \mathbf{N}_{j,i}^L = 0 \quad (6)$$

Where $N_{i,j}$ is the mass transfer rate of component i on stage j.

The general forms for component mass transfer rates across the vapor and liquid films is computed from a diffusive and a convective (bulk-flow) contribution with

$$\mathbf{N}_{j,i}^V = a_j^I \mathbf{J}_{j,i}^V + y_{j,i}\mathbf{N}_{T,j} \quad (7)$$

$$\mathbf{N}_{j,i}^L = a_j^I \mathbf{J}_{j,i}^L + x_{j,i}\mathbf{N}_{T,j} \quad (8)$$

Where a_j^I is total interfacial area for the stage j and $N_{T,j}$ is the total rate on stage j, $\mathbf{N}_{T,j} = \sum_{i=1}^{C} \mathbf{N}_{i,j}$. The diffusive molar fluxes $\mathbf{J}$ are given by (in matrix form):

$$(\mathbf{J}^V) = C_t^V[\kappa^V](\overline{y^V - y^I}) \quad (9)$$

$$(\mathbf{J}^L) = C_t^L[\kappa^L](\overline{x^I - x^L}) \quad (10)$$

Where the $(\overline{y^V - y^I})$ and $(\overline{x^I - x^L})$ are the average mole fraction differences between the bulk and the interface mole fractions. The matrices of Maxwell-Stefan mass transfer coefficients, $[\kappa]$, are calculated for the vapor phase as

$$[\kappa^V] = [\Re^V]^{-1} \tag{11}$$

for a the non-ideal liquid solution as

$$[\kappa^L] = [\Re^L]^{-1}[\Gamma^L] \tag{12}$$

Where $[\Gamma^L]$ is a $(C-1)\times(C-1)$ matrix of thermodynamic factors that corrects for non-ideality, which is a necessary correction for the liquid phase. The $(C-1)\times(C-1)$ Rate Matrix $\Re$ is a matrix of mass transfer resistances calculated from the following formulae:

$$\begin{aligned}
\Re^V_{i,i} &= \frac{y_i}{k^V_{i,C}} + \sum_{k=1,k\neq i}^{C} \frac{y_k}{k^V_{i,k}} \\
\Re^V_{i,j} &= -y_i\left(\frac{1}{k^V_{i,j}} - \frac{1}{k^V_{i,C}}\right) \\
\Re^L_{i,i} &= \frac{x_i}{k^L_{i,C}} + \sum_{k=1,k\neq i}^{C} \frac{x_k}{k^L_{i,k}} \\
\Re^L_{i,j} &= -x_i\left(\frac{1}{k^L_{i,j}} - \frac{1}{k^L_{i,C}}\right)
\end{aligned} \tag{13}$$

Where $k^V_{i,j}$ and $k^L_{i,j}$ are binary pair mass transfer coefficient for each phases. Eqs. (13) are the Maxwell-Stefan equations for mass transfer in multicomponent systems. Mass transfer coefficient is calculated first calculating the matrix function inverted binary diffusion coefficients, $\mathbf{B}$.

$$\begin{aligned}
\mathbf{B}^V_{i,i} &= \frac{y_i}{\mathbf{D}^V_{i,C}} + \sum_{k=1,k\neq i}^{C} \frac{y_k}{\mathbf{D}^V_{i,k}} \\
\mathbf{B}^V_{i,j} &= -y_i\left(\frac{1}{\mathbf{D}^V_{i,j}} - \frac{1}{\mathbf{D}^V_{i,C}}\right) \\
\mathbf{B}^L_{i,i} &= \frac{x_i}{\mathbf{D}^L_{i,C}} + \sum_{k=1,k\neq i}^{C} \frac{x_k}{\mathbf{D}^L_{i,k}} \\
\mathbf{B}^L_{i,j} &= -x_i\left(\frac{1}{\mathbf{D}^L_{i,j}} - \frac{1}{\mathbf{D}^L_{i,C}}\right)
\end{aligned} \tag{14}$$

Where $\mathbf{D}$ is the binary Maxwell-Stefan diffusion coefficient. The Fickian diffusion coefficient matrix [D] is the inverse of the inverted binary diffusion coefficient, $[\mathrm{D}] = [\mathbf{B}]^{-1}$. Matrices [D] and [$\mathbf{B}$] are square matrices of size $(C-1)$. Therefore, the required correlations for mass transfer coefficients for components 1 to $(C-1)$ are expressed using the penetration theory.

The Energy balance equations on stage j are written for each phase as follows:

$$E^V_j = (1+r^V_j)V_jH^V_j - V_{j+1}H^V_{j+1} - F^V_jH^{VF}_j + Q^V_j + e^V_j \tag{15}$$

$$E^L_j = (1+r^L_j)L_jH^L_j - L_{j-1}H^L_{j-1} - F^L_jH^{LF}_j + Q^L_j - e^L_j \tag{16}$$

where H is the enthalpy, Q is the amount of heat added or removed from the system and e_j represents the energy transfer rates for the vapor and liquid phase which are defined by:

$$e^V_j = a^I_j\alpha^V(T^V - T^I) + \sum_{i=1}^{C}\mathbf{N}^V_{i,j}\overline{H}^V_{i,j} \tag{17}$$

$$e^L_j = a^I_j\alpha^L(T^I - T^L) + \sum_{i=1}^{C}\mathbf{N}^L_{i,j}\overline{H}^L_{i,j} \tag{18}$$

Where $\overline{H}_{i,j}$ are the partial molar enthalpies of component i on stage j. There is also a continuity of the energy fluxes across the vapor-liquid interface that gives the interface energy balance:

$$E^L_j = e^V_j - e^L_j \tag{19}$$

Where α^V and α^L are the vapor and liquid heat transfer coefficients respectively, and T^V, T^I, and T^L are the bulk vapor, interface and bulk liquid temperatures. For the calculation of the vapor heat transfer coefficients the Chilton-Colburn analogy between mass and heat transfer is used[24].

Phase equilibrium is assumed to exist only at the interface with the mole fractions in both phases related by:

$$Q^I_{j,i} = \mathrm{K}_{j,i}x^I_{j,i} - y^I_{j,i} = 0 \tag{20}$$

Where $\mathrm{K}_{i,j}$ is the vapor liquid equilibrium ratio for component i, on stage j. The mole fractions must sum to unity in each phase:

$$S^V_j = \sum_{i=1}^{C} y_{j,i} - 1 = 0 \qquad S^L_j = \sum_{i=1}^{C} x_{j,i} - 1 = 0 \tag{21}$$

as well as at the interface

$$S^{VI}_j = \sum_{i=1}^{C} y^I_{j,i} - 1 = 0 \qquad S^{LI}_j = \sum_{i=1}^{C} x^I_{j,i} - 1 = 0 \tag{22}$$

For each stage, the establishment of a liquid hold up on the stage is considered through use of the hydraulic equation for stage pressure drop

$$\Delta P_j = P_{j+1} - P_j \tag{23}$$

Where $P_j = P^V_j = P^L_j$ and ΔP_j is the vapor pressure drop from stage $(j+1)$ to stage j.

The vapor and liquid phases in reactive distillation column are highly nonideal system due to the complex interactions between reaction and distillation. The Poynting correlation is used to calculate the vapor-liquid equilibrium constant. The vapor-liquid equilibrium constant K_i for component i, in the nonideal solution of systems[14, 24], is expressed as

$$\mathrm{K}_{_i} = \gamma_i\frac{\phi^o_i}{\phi^v_i}\frac{P^o_i}{P}\exp\left[\frac{v_i(P-P^o_i)}{RT}\right] \tag{24}$$

Where γ_i is the liquid activity coefficient, ϕ^o_i and ϕ^v_i the vapor fugacity in pure and mixture state respectively, P^o_i the Antoine vapor pressure, v_i the molar volume and P is the total pressure of the system[2]. For the description of liquid phase and gas phase interactions, the Wilson equation model[7] is used while gas phase interactions are modeled using the well

known Peng-Robinson equation[25]. These models are used to calculate liquid activity coefficient γ_i and the vapor fugacity ϕ_i^v (and ϕ_i^o) respectively. These set of nonequilibrium model equations are solved using simultaneous correction method based on Naphtali-Sandholm together with *Newton's* method.

IV. Result and Discussion

The column configuration chosen for the simulations is shown in Fig. 3. This configuration is reported by Jacobs and Krishna[12] for reactive distillation column and many authors have used the same configuration for the standardize of the simulation results. The same configuration is also used in the present study to standardize the computer code developed using MATLAB programming for simulation of equilibrium and nonequilibrium models. In the present study, we have considered the reactive distillation process for *Methyl tert-butyl ether* (MTBE) production. Thermodynamic parameters, transport parameters and reaction kinetics for MTBE production are taken from the literature[12, 24–26].

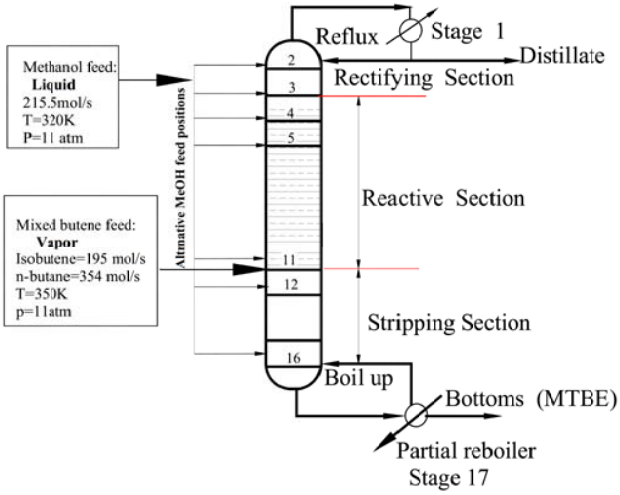

Fig. 3. Configuration of the MTBE synthesis column

The synthesis of MTBE is selected because it is an exothermic and thermodynamically equilibrium limited process. The difficulties are the existence of minimum boiling azeotropes between MTBE-methanol, isobutene-methanol and n-butane-methanol and the separation between n-butane and isobutene, which have close boiling points. The either (MTBE) is derived from isobutene and methanol is blended in gasoline, to increase the octane number and to decrease carbon monoxide emission. The synthesis of MTBE from methanol and isobutene is a reversible exothermic reaction and is catalyzed by Amberlyst 15 or similar ion exchange resin catalyst. The forward reaction is first order with respect to the isobutene concentration and zero order with respect to the methanol concentration. The main side reaction is the dimerization of isobutene to diisobutene and the hydration of isobutene to TBA (tert butyl alcohol). Molar ratio of methanol to isobutene should be higher than 0.8 at each stage to avoid the side reactions.

The Reactive Distillation column considered for simulation consists of 17 stages including a total condenser and partial reboiler. The stages are numbered 1 to 17 from the condenser down to the reboiler. Reactive stages are located in the middle of the column from stage 4 down to stage 11 with Amberlyst 15 ion exchange resin catalyst. The column has also nonreactive sections, a rectification zone (stage 2 to 3) where the inerts are separated, and a stripping zone (stage 12 to16) where the MTBE product is purified. The column has two feed streams: a methanol feed and a mixed butene feed (n-butane and isobutene). A small stoichiometric excess of methanol is used. The methanol feed stage location is varied between stage 2 and stage 16 to study the effect of feed location on MTBE production. The mixed butene feed contains a mixture of isobutene, which is reactive, and n-butane, which is nonreactive or inerts are fed at a stage 11. For standardization the bottom products flow rate is taken as 197 mol/sec, reflux ratio is fixed at 7 and Amberlyst 15 ion exchange resin catalyst loading is taken as $1000 kgs/stage$ from the literature[12]. The reactive distillation column simulation is carried out allowing the variation in feed flow rate, feed location using a user friendly computer code developed with MATLAB programming. The standard values reported in the literature[12] for the production of MTBE in a reactive distillation using number of stages, catalyst loading, flow rates of the phase and reflux ratio are considered for simulation validation as well as model comparison purpose.

A. Validation of Simulation Results

Computer code developed in the present study using MATLAB programming for the simulation of equilibrium and nonequilibrium models are validated using experimental data reported in literature [12] for the reactive distillation column. Table I shows the comparison between experimental data and the simulation results in the present study for equilibrium and nonequilibrium models. It is seen from the table I that the simulation results are in good agreement with the literature data.

TABLE I
Validation of simulation results of Equilibrium (EQ) and Nonequilibrium (NEQ) models

	Experimetal results from litreature[12]		Present study simulation results			
			EQ model		NQ model	
	Flow rate [mol/s]					
Component	Distillate	Bottoms	Distillate	Bottoms	Distillate	Bottoms
isobutene	7.27	1.31	*6.0344*	*0.2157*	7.05556	0.2756
methanol	28.32	0.31	*24.6476*	*0.0006*	25.8858	0.0365
MTBE	0.12	186.74	*0.2594*	*190.919*	0.21747	190.677
n-butane	344.92	8.64	*349.688*	*5.8647*	347.471	6.01125
Total	**380.63**	**197**	**380.63**	**197**	**380.63**	**197**

B. Simulation and Comparison of Concentration Profiles

The simulated concentration profiles of the reactive distillation column using the equilibrium and nonequilibrium modelss are shown in figures 4 to 8. The vapor phase concentration profile using equilibrium model is shown in Fig. 4. The inert component n-butane is observed to be the predominant component in the vapor phase in the rectifying section and reactive

section of the column. High mole fractions of methanol and isobutene are achieved at the bottom part of the reactive section of the column. The liquid phase concentration profile of the components isobutene, methanol, MTBE and the inert n-butane are shown in Fig. 5 for equilibrium model. In the reaction zone from stages 4 to 11 isobutene and methanol are consumed, and maximum mole fractions of methanol and isobutene are observed at the feed locations. The liquid composition profiles show that the liquid is dominated by n-butane from top stage1 to stage 12, thus drastically reducing the rate of reaction. In the stripping section, the liquid quickly becomes richer in MTBE as the mole fraction of the other components decrease because of increasing temperature. In the rectifying section of the reactive distillation column the concentration of MTBE decreases. In the stripping zone, methanol, isobutene and the inert are being separated, resulting in a high concentration of MTBE in the bottoms and high mole fraction of MTBE is obtained in the liquid phase.

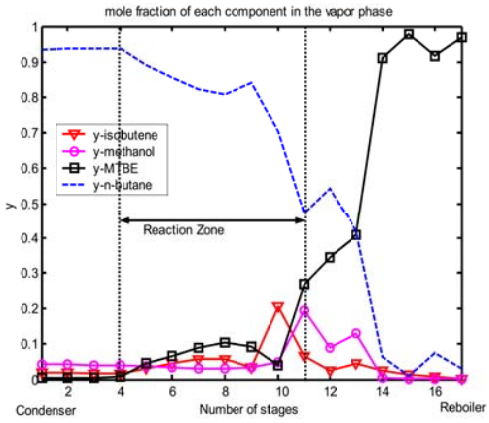

Fig. 4. Concentration profiles using equilibrium model for Vapor Phase

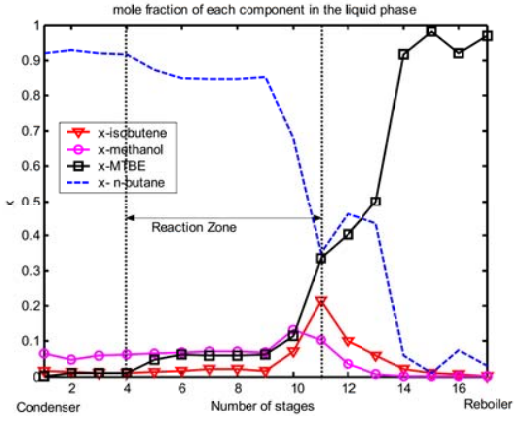

Fig. 5. Concentration profiles using equilibrium model for Liquid Phase

Fig. 6 shows the component mole fraction profiles for the bulk vapor phase obtained using the nonequilibrium model. The predominant component in bulk vapor phase is n-butane. The unreacted methanol is observed in the vapor phase. This is due to its nonideality that it imposes to the system. Methanol is found more concentrated on the upper part of the reactive distillation column and less in the lower part of the column. High concentrations of isobutene are observed at the reaction and separation section of the column in the vapor phase and the Isobutene concentration decreases outside the reaction section of the reactive distillation column in the liquid phase. The drop in isobutene concentration outside the reaction section in the liquid phase is due to equilibrium limitation between the liquid and vapor phase, and bottom of the section is more predominant with MTBE and the top section is with methanol. The higher concentrations of isobutene in both the reactive and non reactive sections in the vapor phases may need further study to explain this behavior. A sharp increase of MTBE concentration is observed in the stripping section reaching maximum at the last stage (reboiler). Similar trend is observed for liquid phase concentration profiles shown in Fig. 7. The concentration of MTBE decreases in the rectifying section and increases in the stripping section.

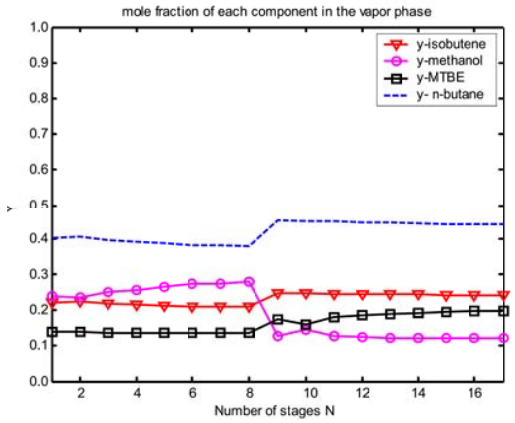

Fig. 6. Concentration profiles using nonequilibrium model for Vapor Phase

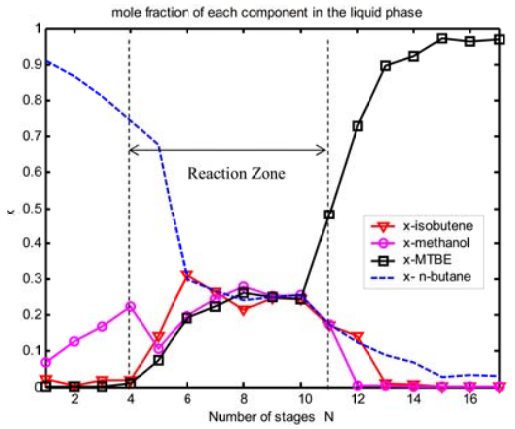

Fig. 7. Concentration profiles using nonequilibrium model for Liquid Phase

Fig. 8 shows the comparison between equilibrium and nonequilbrium models for the mole fraction of MTBE in the liquid phase. Both the model simulation results give similar

trends. In the reactive and stripping section higher mole fraction of MTBE is obtained by nonequilibrium model than by equilibrium model. The observed differences among the profiles are due to direct account of interface heat and mass transfer in nonequilibrium model for more MTBE production.

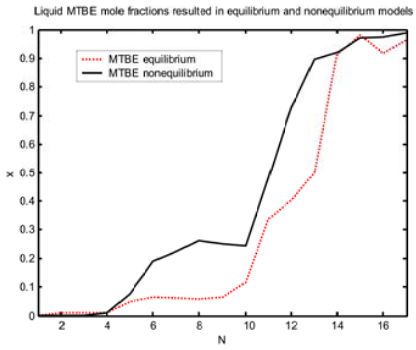

Fig. 8. Comparison of concentration profile of MTBE for equilibrium and nonequilibrium model simulations.

Fig. 9 shows the composition profile for isobutene (IB), methanol (MeOH), in the liquid phase of both equilibrium and nonequilibrium models. The concentration profile of these reactants resulted from equilibrium model shows a maximum concentration at their respective feed stage and then decrease as we go away either up or down from that stage. Whereas the profiles obtained by nonequilibrium model shows that concentrations are high in reactive section of the column

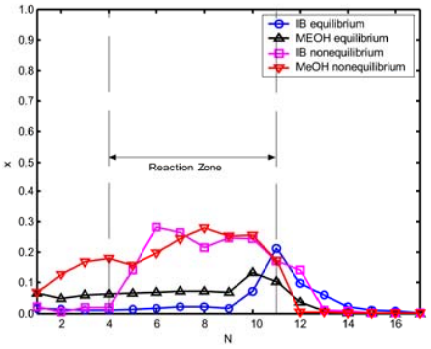

Fig. 9. Comparison of concentration profile of reactants for equilibrium and nonequilibrium model simulations for IB & MeOH.

C. Simulation and Comparison of Temperature Profiles

The simulated temperature profiles of the reactive distillation column obtained from both the models are shown in Fig. 10. A smooth temperature profile is observed with equilibrium model for vapor phase showing lower temperature in the rectifying section and gradually increasing to a maximum value in the stripping section. As the reaction equilibrium constant increases exponentially with decreasing temperature, the equilibrium is shifted toward MTBE in the reaction zone, located at the middle of the column from stages 4 to 11. The larger temperatures in the bottom are due to the presence of MTBE, which has a significantly higher molecular weight and higher boiling temperature. On can see from Fig. 10 the simulated temperature profiles obtained using nonequilibrium model for bulk liquid temperature, bulk vapor temperature and for vapor-liquid interphase. It is seen from the figure that the bulk vapor temperatures are higher than the bulk liquid temperatures, and interphase temperatures are in between approaching the theoretical behavior.

A comparison between the equilibrium and nonequilibrium models for the prediction of temperature profile is shown in Fig. 10 for the bulk vapor and bulk liquid phases. It is observed that the stage temperature profile of equilibrium model is identical with the bulk liquid temperature of the nonequilibrium model. It is also seen from the figure that the bulk vapor temperatures of the nonequilibrium model is higher than the equilibrium model stage temperature. This is because thermal equilibrium assumption of the equilibrium model forces the liquid and vapor leaving a stage to have the same temperature but in reality heat transfer between the two phases is limited.

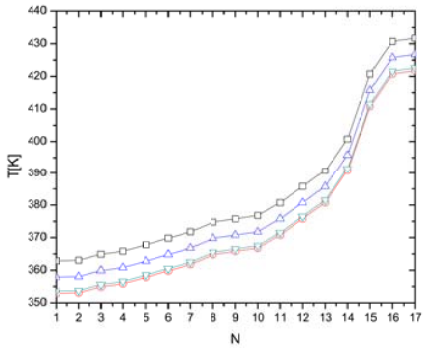

Fig. 10. Comparison of temperature profiles resulted from equilibrium and nonequilibrium models.(a) from nonequilibrium model bulk vapor temperate, T^V, (□), bulk liquid temperate, T^L, (○) and vapor-liquid interface temperature, T^I, (△). (b) the equilibrium model stage temperature (▽)

D. Simulation and Comparison of Reaction Rate Profiles

The simulated results for the rate of formation of MTBE in the reaction zone is shown in Fig. 11 for both models. The reactants methanol and isobutene and n-butane mixture are introduced on stage 10 and stage 11 respectively. It is seen from Fig. 11 that there is no formation of MTBE in the non-reactive sections. It is also observed that the reaction rate increases starting from stage 4 to stage 10 and reaches maximum at stage 11 and shows that the forward reaction dominates on every stage of the reactive section.

The rate of reaction profiles obtained for the models are compared in Fig. 11. The reaction rate profile for equilibrium model is smooth compared to the nonequilibrium model simulation. The instability of the reaction rate profile is mainly due to the complex interaction of reaction and separation process together with the nonideality of the system that are directly considered on developing the nonequilibrium stage model. The higher reaction rate for nonequilibrium model may be

attributed to the higher temperature of the bulk phase with the relaxation of the thermal equilibrium.

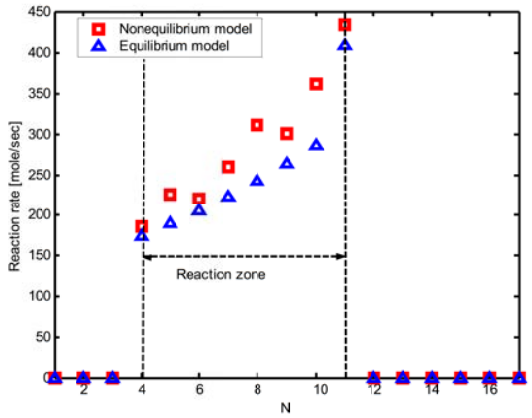

Fig. 11. Comparison of reaction rate profiles of formation of MTBE using equilibrium and nonequilibrium models.

E. Sensitivity Analysis

The sensitivity analysis have been conducted for the influences of methanol feed stage location and reflux ratio on the isobutene conversion. The feed ratios and concentrations are not considered because if the molar ratio of methanol to isobutene is lower than 0.8 at each stage, the main side reactions are the dimerization of isobutene to diisobutene and the hydration of isobutene to tert-butyl-alcohol(TBA). The molar ratios of the feed methanol to isobutene was maintained above 0.8 taking a small excess of stoichiometric concentrations of methanol.

1) Comparison of Isobutene Conversion: Effect of Methanol Feed Location : A series of simulation runs were carried out with varying methanol feed stage location from stage 2 to 16. First the column temperature and concentration profile were calculated with the methanol feed point located at stage 2. Then the values obtained from this simulation were used as initial values for the calculations with the methanol feed point located at stage 3 using the same operating and feed conditions as in the previous simulation. The concentration and temperature profile thus obtained were used for the simulation with the methanol feed point at stage 4 and so on until stage 16.

The simulation results for isobutene conversion using the equilibrium and nonequilibrium models are shown in figure 12. The difference in isobutene conversion between the models with methanol feed location is small in the rectifying and reactive sections. Moving the methanol feed from stage 11 to stage 12 in the stripping section, the isobutene conversion drops to a lower value with the equilibrium model where as the drop with nonequilibrium model is much smaller. This is due to introduction of mass transfer resistance in the nonequilibrium model and also the existence of methanol in the vapor form in the stripping section.

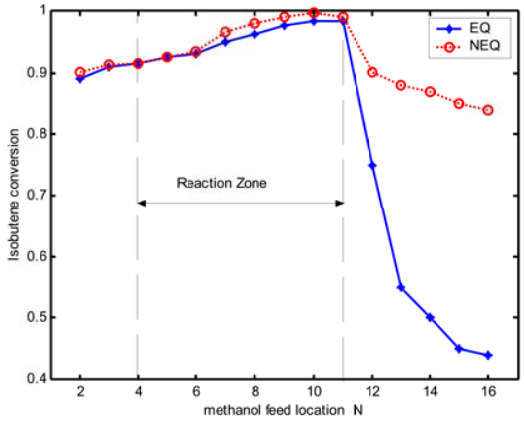

Fig. 12. Comparison of Isobutene conversion with methanol feed location with the equilibrium and nonequilibrium models

2) Comparison of Isobutene Conversion: Effect of Reflux Ratio: The effect of the reflux ratio, R on the isobutene conversion in the reactive distillation column was determined by varying the reflux ratio from 1 to 10. This ratio is chosen because no significant variation in the conversion of isobutene is observed beyond 10 and the conversion lowers below 1. For each value of reflux ratio the steady-state column concentration and temperature profiles were calculated. The simulated results of isobutene conversion with reflux ratio is shown in figure 13 for both the models. It is observed from the figure that the conversions of isobutene increases with increase in reflux ratio up to 4.5 and becomes independent for further rise in reflux ratio.

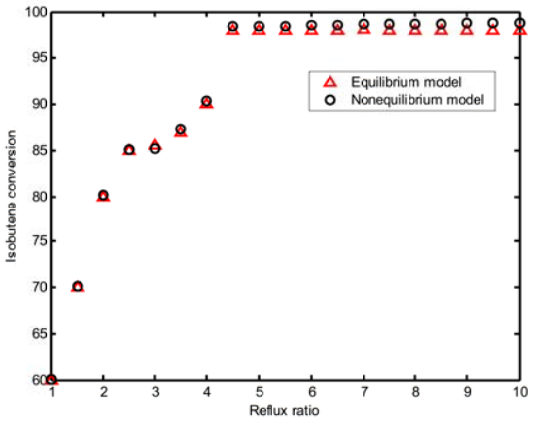

Fig. 13. Comparison of isobutene conversion with reflux ratio for equilibrium and nonequilibrium models.

V. Conclusions

Reactive Distillation is an attractive alternative to the classical combination of reactors and separators. The simulation studies are carried out using the equilibrium and nonequilibrium models for the MTBE system using the computer code developed in the present study with MATLAB programming. Both the equilibrium and nonequilibrium models show similar

trend for concentration, temperature and reaction rate profiles in the reactive and separation sections. The MTBE concentration, the bulk vapor temperatures and reaction rates are higher with nonequilibrium model compared to equilibrium model. This is due to incorporation of reaction rates and mass transfer flux in the nonequilibrium models. The column operating performance depends on feed location, and reflux ratio. The drop in isobutene conversion with nonequilibrium model prediction is much smaller than the equilibrium model in the stripping section. Introduction of methanol feed in the stripping section is supposed to give higher conversion because of the nature of the feed, which is well predicted by the nonequilibrium model demonstrating the superiority over equilibrium modeling approach closer to the experimental data reported in the literature.

REFERENCES

[1] A. Higler, R. Krishna, J. Ellenberger, and R. Taylor, "Counter-current operation of of a structured catalytically packed bed reactor: Liquid phase mixing and mass transfer," *Chem. Eng. Sci.*, vol. 54, pp. 5145–5152, 1999.

[2] A. Higler, R. Krishna, and R. Taylor, "A nonequilibrium cell model for multicomponent(reactive) separation processes," *AIChE. J.*, vol. 45, pp. 2357–2363, 1999.

[3] A. A. Kiss, F. Omota, A. C. Dimian, and G. Rothenberg, "The heterogeneous advantage: Biodiesel by catalytic reactive distillation," *Top. Catal.*, vol. 40, pp. 141–150, 2006.

[4] A. Higler, R. Krishna, and R. Taylor, "Nonequilibrium modeling of reactive distillation: A dusty fluid model for heterogeneously catalyzed processes," *Ind. Eng. Chem. Res.*, vol. 39, pp. 1696–1707, 2000.

[5] A. A. Kiss, A. C. Dimian, and G. Rothenberg, "Biodiesel by catalytic reactive distillation powered by metal oxides," *Energy Fuels*, vol. 22, pp. 598–604, 2008.

[6] G. J. Harmsen, "Reactive distillation: The front-runner of industrial process intensification a full review of commercial applications, research, scale-up, design and operation," *Chem. Eng. Process.*, vol. 46, pp. 774–780, 2007.

[7] H. S. Eldarsi and P. L. Douglas, "Methyl-tert-butyl-ether catalytic distillation column: part I: Multiple steady states," *Chem. Eng. Res. Des.*, vol. 76, pp. 509–516, 1998.

[8] R. S. Huss, F. Chen, M. F. Malone, and M. F. Doherty, "Reactive distillation for methyl acetate production," *Comput. Chem. Eng.*, vol. 27, pp. 1855– 1866, 2003.

[9] F. I. Gómez-Castro, V. Rico-Ramírez, J. G. Segovia-Hernández, S. Hernández-Castro, G. González-Alatorre, and M. M. El-Halwagi, "Simplified methodology for the design and optimization of thermally coupled reactive distillation systems," *Ind. Eng. Chem. Res.*, vol. 51, pp. 11 717–11 730, 2012.

[10] Y. Jiao, S.-J. Wang, K. Huang, H. Chen, and W. Liu, "Design and analysis of internally heat-integrated reactive distillation processes," *Ind. Eng. Chem. Res.*, vol. 51, pp. 4002–4016, 2012.

[11] R. Gani, T. S. Jepsen, and E. S. Pérez-Cisneros, "A Generalized Reactive Separation Unit Model. Modelling and Simulation Aspects," *Comput. Chem. Eng.*, vol. 22, pp. 363–370, 1998.

[12] R. Jacobs and R. Krishna, "Multiple solutions in reactive distillation for methyl tert-butyl ether synthesis," *Ind. Eng. Chem. Res.*, vol. 32, pp. 1706–1709, 1993.

[13] L. U. Kreul, A. Gorak, and P. I. Barton, "Modelling of homogeneous reactive separation processes in packed columns," *Chem. Eng. Sci.*, vol. 54, pp. 19–25, 1999.

[14] X. Xu, Y. Zheng, and G. Zeng, "Kinetics and effectiveness of catalyst for synthesis of Methyl-Tert-Butyl-Ether in catalytic distillation," *Ind. Eng. Chem. Res.*, vol. 34, pp. 2232–2236, 1995.

[15] R. S. Kamath, Zhiwen, K. Sundmacher, P. Aghalayam, and S. M. Mahajani, "Process analysis for dimerization of isobutene by reactive distillation," *Ind. Eng. Chem. Res.*, vol. 45, pp. 1575–1582, 2006,.

[16] W. Hung, I. Lai, Y. Chen, S. Hung, H. Huang, M. Lee, and C. Yu, "Process chemistry and design alternatives for converting dilute acetic acid to esters in reactive distillation," *Ind. Eng. Chem. Res.*, vol. 45, pp. 1722–1733, 2006.

[17] M. Wang, H. Wang, N. Zhao, Wei, and Y. Sun, "High-yield synthesis of dimethyl carbonate from urea and methanol using a catalytic distillation process," *Ind. Eng. Chem. Res.*, vol. 46, pp. 2683–2687, 2007.

[18] R. Baur and R. Krishna, "Hardware selection and design aspects for reactive distillation columns. A case study on synthesis of TAME," *Chem. Eng. Process.*, vol. 41, pp. 445–462, 2002.

[19] A. Katariya, K. Moudgalya, and S. Mahajani, "Nonlinear dynamic effects in reactive distillation for synthesis of TAME," *Ind. Eng. Chem. Res.*, vol. 45, pp. 4233 – 4242, 2006.

[20] Y. H. Jhon and T. Lee, "Dynamic simulation for reactive distillation with ETBE synthesis," *Sep. Purif. Technol.*, vol. 31, pp. 301–317, 2003.

[21] J. D. Seader and J. E. Henley, *Separation process principles*. John Wiley and Sons, Inc, 1998.

[22] R. Taylor and R. Krishna, "Modeling reactive distillation," *Chem. Eng. Sci.*, vol. 55, pp. 5183–5229, 2000.

[23] A. Gezae, "Modeling and simulation of reactive distillation," Master's thesis, Department of Chemical Engineering, Faculty of Technology, School of Graduate Studies, Addis Ababa University, July 2004.

[24] R. C. Reid, J. M. Prausnitz, and B. M. Poling, *The properties of gases and liquids*. New York: McGraw-Hill, 1988.

[25] J. M. Smith, H. C. V. Ness, and M. M. Abbot, *Introduction to chemical engineering thermodynamics*. McGraw-Hill Book Company, Inc, 1996.

[26] R. K. Sinnott, *Coulson & Richrdson's: Chemical engineering design*. Butterworth, 2005, vol. 6.